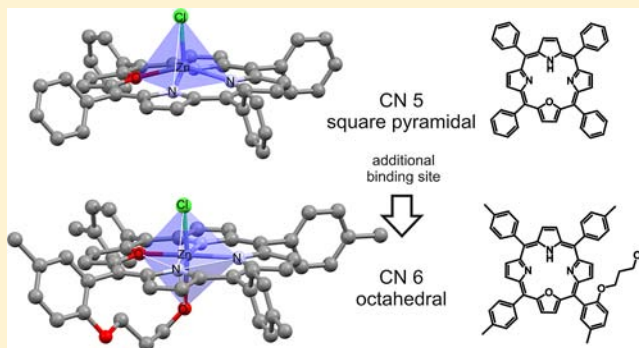


## Molecular Structure, UV/Vis Spectra, and Cyclic Voltammograms of Mn(II), Co(II), and Zn(II) 5,10,15,20-Tetraphenyl-21-oxaporphyrins

Silvio Stute,<sup>†</sup> Linda Götzke,<sup>†</sup> Dirk Meyer,<sup>†</sup> Mohamed L. Merroun,<sup>‡</sup> Peter Rapta,<sup>§,||</sup> Olga Kataeva,<sup>⊥</sup> Wilhelm Seichter,<sup>#</sup> Kerstin Gloe,<sup>†</sup> Lothar Dunsch,<sup>§</sup> and Karsten Gloe<sup>\*,†</sup><sup>†</sup>Department of Chemistry and Food Chemistry, TU Dresden, 01062 Dresden, Germany<sup>‡</sup>Institute of Resource Ecology, Helmholtz Center Dresden-Rossendorf, 01314 Dresden, Germany<sup>§</sup>Center of Spectroelectrochemistry, Leibniz Institute for Solid State and Materials Research, 01171 Dresden, Germany<sup>||</sup>Institute of Physical Chemistry and Chemical Physics, Slovak University of Technology, 81237 Bratislava, Slovak Republic<sup>⊥</sup>A. E. Arbutov Institute of Organic and Physical Chemistry, Kazan 420088, Russia<sup>#</sup>Institute of Organic Chemistry, TU BA Freiberg, 09596 Freiberg, Germany

## S Supporting Information

**ABSTRACT:** The 5,10,15,20-tetraphenyl-21-oxaporphyrin complexes of Mn(II), Co(II), and Zn(II) have been crystallized and studied by X-ray diffraction, NMR and UV/vis spectroscopy, and mass spectrometry as well as cyclic voltammetry. The X-ray structure of the earlier described Cu(II) complex is also reported. All complex structures possess a five-coordinate, approximately square-pyramidal geometry with a slight deviation of the heteroaromatic moieties from planarity. The packing structures are characterized by parallel strands of complex molecules interacting by weak hydrogen bonds. In the case of Zn(II) an octahedral complex has also been isolated using a side-chain hydroxy functionalized oxaporphyrin ligand; the structure was verified by NMR and EXAFS spectroscopy. Cyclic voltammetry studies reveal that the reduction of the complex bound Mn(II), Co(II), and Zn(II) ions is a ligand-centered process whereas the first oxidation step depends on the metal ion present.



## ■ INTRODUCTION

Due to its ability to form highly stable, noncharged complexes with divalent cations, the porphyrin core is one of the most investigated ligand systems for metal complexation.<sup>1</sup> Over the years several modifications of porphyrins led to various new structures enlarging the field of porphyrin chemistry.<sup>2</sup> Specifically, replacement of one or more pyrrole nitrogen atoms affects the electronic structure of the ring system. This core modification can be achieved, for example, by inversion<sup>3,4</sup> or substitution<sup>5–17</sup> of one or more pyrrole rings. The introduction of heterocycles other than pyrrole results in the formation of the so-called heteroporphyrins, in which one or more nitrogen atoms are replaced by phosphorus<sup>5–7</sup> or an element of group 16 (O, S, Se, Te).<sup>9–17</sup> The insertion of chalcogene atoms in the macrocyclic ring leads not only to the alteration of the donor set and the ring size but also to the lack of at least one core proton. These changes dramatically influence characteristic properties such as aromaticity and metal binding ability of the porphyrins.<sup>9,11,18</sup> While thiophene and its Se or Te containing analogues cause a decrease in the size of the cavity, oxaporphyrins and regular porphyrins have almost identical cavity.<sup>9,19</sup> At present only a few papers on Fe(II/III),<sup>20,21</sup> Ni(I/II),<sup>16,22–26</sup> Cu(I/II),<sup>16,26,27</sup> Zn(II),<sup>16,28</sup> and

Re(I)<sup>29</sup> oxaporphyrin complexes have been published. It is interesting to note that the spectral, magnetic, and electrochemical properties of Cu(II) oxaporphyrins have been studied,<sup>16,26,27</sup> but an X-ray structural characterization is missing. Also the formation of Co(II) and Mn(II) complexes has been shown only spectroscopically.<sup>16</sup> Recently results on Zn(II) complexes with a series of various *meso*-substituted oxaporphyrins, including a crystal structure, have been published.<sup>28</sup>

To gain more insight into the binding pattern of 21-oxaporphyrins, we report here the synthesis and characterization of Mn(II), Co(II), Cu(II), and Zn(II) complexes with the 5,10,15,20-tetraaryl-21-oxaporphyrins 1–3.

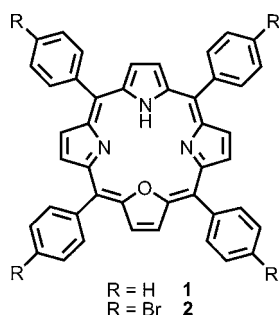
## ■ RESULTS AND DISCUSSION

Symmetric 5,10,15,20-tetraaryl-21-oxaporphyrins (1, 2) (Scheme 1) and the asymmetric oxaporphyrin bearing a side chain with an additional donor function (3) (Scheme 2) were used for metal binding experiments. According to the literature,

Received: October 16, 2012

Published: January 14, 2013

Scheme 1. Oxaporphyrins Studied



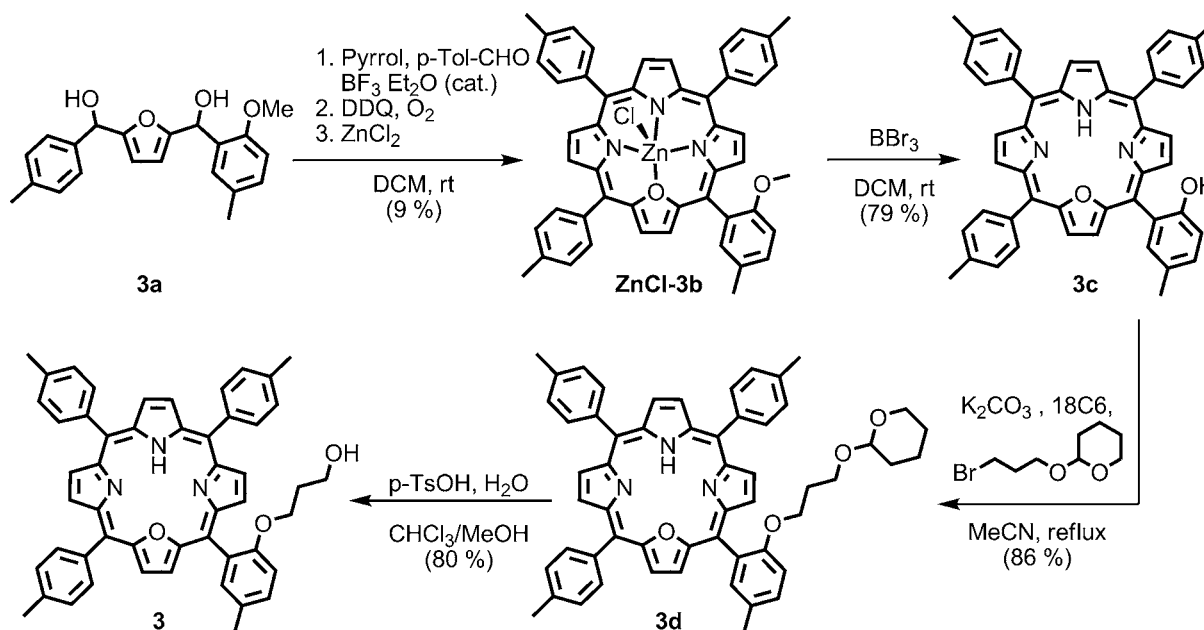
the closure of the macrocycle was achieved by condensation of a 2,5-bis(arylhydroxymethyl)-furan (**1a–3a**) with pyrrol and an arylaldehyde.<sup>22</sup> For the synthesis of the asymmetric oxaporphyrin **3** further steps were necessary to introduce the additional hydroxyl donor function. The cyclization reaction with the asymmetric 2-[(2-methoxy-5-methylphenyl)hydroxymethyl]-5-[(*p*-tolyl)hydroxymethyl]-furan (**3a**) afforded an oxaporphyrin containing a single methoxy group (**3b**). As the separation of oxaporphyrins is often difficult because of their high basicity,<sup>22</sup> the formation of the Zn(II) complex was used to improve the separation behavior in chromatographic isolation. In contrast to the commonly used chromatography employing the free base porphyrin on basic aluminum oxide<sup>17,30</sup> which results in broadened fractions and significantly reduced yields, this procedure leads to a more defined product fraction with an enhanced separation from impurities. The conversion of the methoxy group into a hydroxyl group with concomitant dissociation of the Zn(II) complex was achieved under standard ether cleavage conditions. Subsequent etherification with a 3-propanol synthon and cleavage of the protecting group gave the desired pentadentate oxaporphyrin **3**.

The formation of all metal complexes was accomplished by refluxing the oxaporphyrin and an appropriate metal chloride in chloroform or a chloroform/methanol mixture. After purifica-

tion by chromatography and recrystallization, the desired metalloporphyrins were obtained in almost quantitative yields. In addition to the known Cu(II) complex<sup>26</sup> we inserted Co(II) (**CoCl-1**) and Mn(II) (**MnCl-1**) into ligand **1**. In the case of Zn(II) several complexes (**ZnCl-1**, **ZnClO<sub>4</sub>-2**, **ZnCl-3**) were synthesized. The product metallooxaporphyrins are stable in the solid and solution.

Crystallization of Mn(II), Co(II), Zn(II), and Cu(II) 21-oxaporphyrins from chloroform/*n*-heptane or ethyl acetate afforded crystals suitable for X-ray diffraction (Figure 1, Table 1). All complexes possess a five-coordinate, square pyramidal geometry with chloride in the axial position. The metal atoms are shifted out of the plane of the porphyrin donor atoms toward the chloride. The metal–nitrogen distances are all elongated compared to their four-coordinate<sup>31–34</sup> and five-coordinate<sup>31,35–38</sup> N<sub>4</sub>-analogues. The furan ring coordinates in an  $\eta^1$  fashion via the oxygen with M–O distances similar to ether oxygen–metal bonds.<sup>39–42</sup> In general, the exact assignment of the heteroatoms is difficult due to almost identical carbon–oxygen and carbon–nitrogen distances. However, the problem could be solved on the basis of the relative peak intensities of the heteroatoms as well as the metal–donor distances. In case of **ZnCl-1** the attempt to refine with disordered oxygen and nitrogen atoms in positions 21 and 23 afforded no significant improvement of the structure quality, and the anisotropic refinement failed. For the Mn(II) complex the refinement of the structure with no disorder showed larger vibrational parameters for the oxygen atom and smaller vibrational parameters for one of the nitrogen atoms. Moreover, additional peaks of different electron density appeared near this N-atom, typical for wrong assignment of the atom types. When the positions of the O and N atom were interchanged, the same picture was observed. Thus two opposite atoms O and N were refined with positional disorder approximately 60 to 40%. The R-factor decreased by 0.004 for disordered structure in comparison with nondisordered structure. The other two nitrogen atoms showed no indication of disorder and in the final structure  $U(\text{eq.})$  were very similar for all four donor atoms.

Scheme 2. Synthetic Route for the Synthesis of Oxaporphyrin 3



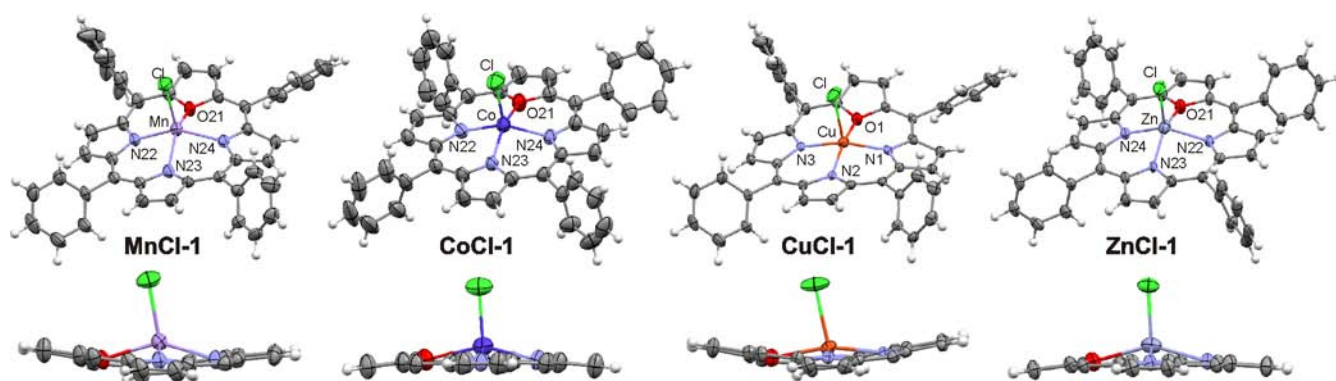


**Figure 1.** Perspective (top) and side (bottom) views on the X-ray structures of the Mn(II), Co(II), Cu(II), and Zn(II) complexes of **1**; phenyl rings are omitted in the side views.

**Table 1.** Crystallographic Data for MnCl-1, CoCl-1, CuCl-1, and ZnCl-1

	MnCl-1	CoCl-1	CuCl-1	ZnCl-1
formula	C <sub>45</sub> H <sub>29</sub> Cl <sub>4</sub> MnN <sub>3</sub> O	C <sub>44</sub> H <sub>28</sub> ClCoN <sub>3</sub> O	C <sub>45</sub> H <sub>29</sub> Cl <sub>4</sub> CuN <sub>3</sub> O	C <sub>44</sub> H <sub>28</sub> ClN <sub>3</sub> OZn
formula weight	824.45	709.07	833.06	715.53
T [K]	293	293	153	153
λ [Å]	0.71073	0.71073	0.71073	0.71073
space group	P2 <sub>1</sub> /n (No. 14)	P2 <sub>1</sub> /n (No. 14)	P2 <sub>1</sub> /n (No. 14)	P2 <sub>1</sub> /n (No. 14)
a [Å]	12.142(2)	10.162(1)	12.0352(3)	9.9737(3)
b [Å]	22.300(1)	15.936(1)	21.9674(6)	15.8831(5)
c [Å]	14.460(3)	20.933(1)	14.4403(4)	20.9518(5)
α	90°	90°	90°	90°
β	102.65(1)°	90.61(1)	102.788(1)°	90.539(2)°
γ	90°	90°	90°	90°
V [Å <sup>3</sup> ]	3820.2(10)	3389.7(4)	3723.06(17)	3318.90(16)
Z	4	4	4	4
D <sub>calcd</sub>	1.433	1.390	1.486	1.432
μ [mm <sup>-1</sup> ]	0.666	0.626	0.915	0.862
R <sup>a</sup>	0.0873	0.0461	0.0571	0.0450
R <sub>w</sub> <sup>b</sup>	0.2314	0.1152	0.1355	0.1081

$$^a R = \sum \| |F_o| - |F_c| \| / \sum |F_o|. \quad ^b R_w = [\sum w \cdot (F_o^2 - F_c^2) / \sum w (F_o^2)^2]^{1/2}.$$

Similar disorders have already been reported.<sup>22,28</sup> As this precludes a precise assignment, the metal–O and metal–N distances are only listed as metal–donor distances in Table 2. All M–Cl distances are in the typical range<sup>22,28,43–45</sup> with these bonds almost perpendicular to the plane of the donor atoms. The largest deviations from the vertical occur in **MnCl-1** and **CuCl-1** with angles of 78.9° and 79.2°, respectively. While the values of the bond lengths and angles in **ZnCl-1** are in good accordance with those in the Zn(II) oxaporphyrin complex

**Table 2.** Selected Distances (Å) in the Complexes of **1** Compared with Literature Data

	M–D <sup>a</sup>	M–Cl	M plane <sup>b</sup>	X plane <sup>c</sup>
<b>MnCl-1</b>	2.13, 2.14, 2.16, 2.20	2.33	0.66	0.18
<b>CoCl-1</b>	2.05, 2.08, 2.10, 2.22	2.25	0.53	0.05
<b>CuCl-1</b>	2.01, 2.04, 2.05, 2.14	2.37	0.32	0.20
<b>ZnCl-1</b>	2.07, 2.10, 2.15, 2.24	2.22	0.61	0.05
<b>ZnCl-OTMPP</b> <sup>28</sup>	2.08, 2.09, 2.11, 2.19	2.21	0.59	0.15
<b>NiCl-ODPDTP</b> <sup>22</sup>	2.00, 2.01, 2.06, 2.18	2.29	0.33	0.19

<sup>a</sup>Distance between metal center and donor atoms of the oxaporphyrin (N<sub>3</sub>O). <sup>b</sup>Distance between metal center and the plane defined by the four inner core atoms (N<sub>3</sub>O). <sup>c</sup>Average atomic deviation from the mean plane defined by the 24 atoms of the porphyrin.

**ZnCl-OTMPP**<sup>46</sup> having methoxycarbonyl functions in para-position of meso-phenyl rings,<sup>28</sup> the conformation of the porphyrin core differs. In contrast to **ZnCl-OTMPP** adopting a ruffled conformation, **ZnCl-1** shows a “doming” with a significant smaller deviation from the mean plane (average atomic deviation of 0.05 Å). Despite the metal center being a little closer to the plane of the donor atoms, **CoCl-1** is isostructural with **ZnCl-1** and the porphyrin core shows a doming distortion with the same average atomic deviation. **CuCl-1** and **MnCl-1** are also isostructural and exhibit a saddle distortion like the Ni(II) complex<sup>22</sup> **NiCl-ODPDTP**.<sup>47</sup> Each of these three complexes contain a disordered solvent molecule within the crystal, namely, chloroform (**CuCl-1**, **MnCl-1**) or dichloromethane (**NiCl-ODPDTP**), that forms a weak hydrogen bond<sup>48</sup> (2.40 Å, 2.34 Å, 2.87 Å) to the chloride ligand (M–Cl⋯HCR<sub>3</sub>). The proximity of the bulky –CCl<sub>3</sub> residue, which is induced by this H-bond, might contribute to the greater deviation of the chloride ligand from the vertical in **CuCl-1** and **MnCl-1**.

The crystal packing of **CuCl-1** and **MnCl-1** is characterized by parallel strands of complex molecules along the *c*-axis overlapping their inverted forms (Figure 2a). The chlorides of the pairs of inverted molecules are pointing away from each other, and the porphyrin plane distances are 3.77 Å and 3.85 Å, respectively. In contrast, no overlapping pairs of porphyrin

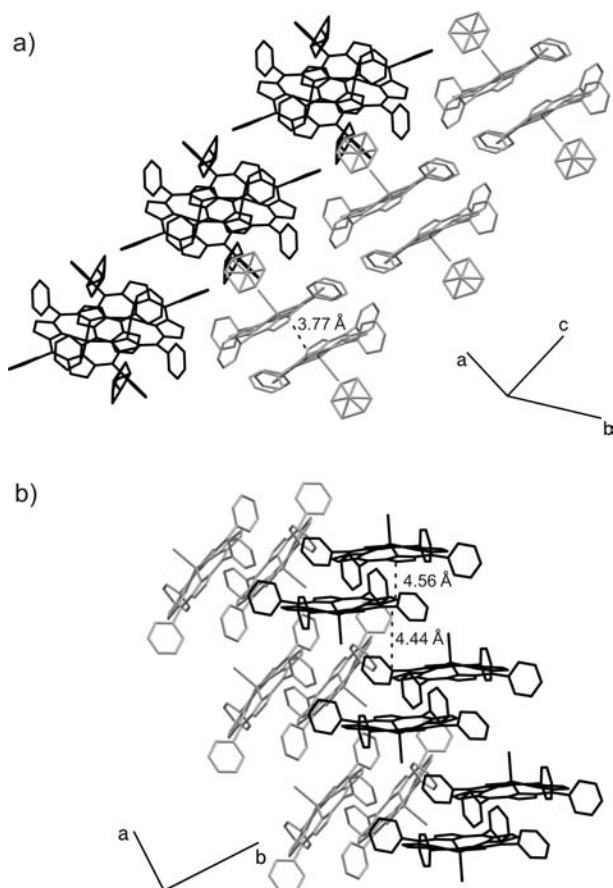


**Figure 2.** Molecular packing of (a) **CuCl-1** including the disordered chloroform molecules and (b) **ZnCl-1**. The gray and black molecules are related by a 2-fold screw axis along the *b*-axis. Hydrogen atoms are omitted for clarity.

rings can be found in **CoCl-1** and **ZnCl-1**. The complex molecules are stacked along the *a*-axis alternating with their inverted form with the shortest porphyrin plane distances of 4.57 Å and 4.44 Å, respectively (Figure 2b). Besides the previously mentioned hydrogen bonds with an attached solvent molecule, the chloride interacts with hydrogen atoms on neighboring molecules. So, in all four complex structures one or two weak hydrogen bonds are formed with CH...Cl distances in the range of 2.77–2.95 Å. In general, only a small number of weak CH– $\pi$  interactions are observed (distances between 2.64 and 3.00 Å).

The electronic spectra of **MnCl-1**, **CoCl-1**, and **ZnCl-1** (Figure 3, Table 3) resemble the spectra of the five-coordinate oxaporphyrin complexes with iron(II),<sup>20</sup> copper(II),<sup>26</sup> and zinc(II).<sup>28</sup> They show three Q-bands and a splitting of the Soret band, which can be easily explained by the decreased symmetry with respect to the metal complexes of the regular porphyrins.<sup>49</sup> Expectedly, the electronic spectrum of **ZnCl-1** coincides well with the spectrum of **ZnCl-OTMPP**<sup>28,46</sup> having an average hypsochromic shift of 5–9 nm.

The redox chemistry of the present metal porphyrins was followed by cyclic voltammetry (Figure 4, Table 4). It is known that the  $E_{1/2}$  values depend on the number and the nature of donor atoms in the porphyrin core.<sup>14,50</sup> In general, the reduction potentials are raised to more positive values on replacement of nitrogen by oxygen or sulfur. However, the

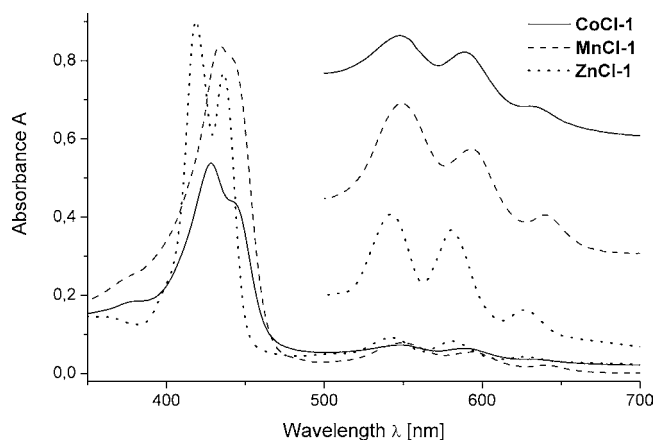


**Figure 3.** Electronic absorption spectra of **MnCl-1**, **CoCl-1**, and **ZnCl-1** in  $\text{CH}_2\text{Cl}_2$  including 5-fold magnification of the Q-bands.

**Table 3.** Electronic Spectral Data for the Metal Complexes of **1** in  $\text{CH}_2\text{Cl}_2$

	Soret bands $\lambda$ [nm] ( $\epsilon$ [ $10^3$ $\text{M}^{-1}\cdot\text{cm}^{-1}$ ])	Q-bands $\lambda$ [nm] ( $\epsilon$ [ $10^3$ $\text{M}^{-1}\cdot\text{cm}^{-1}$ ])
<b>MnCl-1</b>	434 (101), 442 sh (97)	549 (10), 593 (7), 640 (3)
<b>CoCl-1</b>	428 (108), 444 sh (87)	548 (15), 588 (13), 635 (7)
<b>CuCl-1</b> <sup>26</sup>	416, 430	534, 572, 625
<b>ZnCl-1</b>	419 (180), 436 (154)	542 (18), 580 (17), 627 (8)
<b>ZnCl-OTMPP</b> <sup>28</sup>	426 (174), 442 (151)	547 (11), 588 (10), 636 (3)

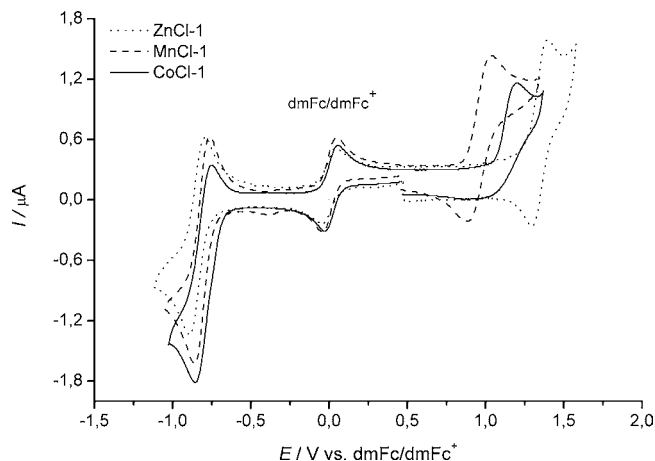


**Figure 4.** Cyclic voltammograms for **ZnCl-1**, **MnCl-1**, and **CoCl-1** in dichloromethane at a Pt electrode and a scan rate of  $100 \text{ mV s}^{-1}$ . The voltammetric curve of ligand **1** is not displayed.

**Table 4.** Electrochemical Data for the First Electron Transitions of **1** and Its Metal Complexes

	$E_{1/2}^1$ (red.) [V] vs $E_{1/2}^1$ (dmFc)	$E_{1/2}^1$ (ox.) [V] vs $E_{1/2}^1$ (dmFc)	$\Delta E_{1/2}^1$ [V]
<b>1</b>	−1.04(−1.11)	1.14 (1.07)	2.18
<b>ZnCl-1</b>	−0.84 (−0.91)	1.34 (1.27)	2.18
<b>CoCl-1</b>	−0.82 (−0.89)	1.17 <sup>a</sup> (1.10)	1.99
<b>MnCl-1</b>	−0.82 (−0.89)	0.97 (0.90)	1.79

<sup>a</sup>Irreversible values in brackets calcd. vs SCE data obtained on Pt wire working electrode under inert conditions and recorded at  $100 \text{ mV s}^{-1}$  scan speed in 0.2 M TBAPF<sub>6</sub>/ $\text{CH}_2\text{Cl}_2$  with dmFc as internal standard.



influence of the metal ions Mn(II), Co(II), and Zn(II) on reduction potentials is not as distinct as that of the ligand.

In the literature the first reduction of the complexes is discussed either as a metal-centered [M(II)–M(I)] or ligand-centered one-electron transfer.<sup>20,26</sup> The potential of the first reduction of free base oxaporphyrin **1** is at  $-1.04$  V. The half-wave potentials of **MnCl-1**, **CoCl-1**, and **ZnCl-1** are nearly identical and are in accordance with the second half-wave potential of **FeCl<sub>2</sub>-1**<sup>20</sup> ( $-0.895$  V). Thus, a ligand-centered reduction seems most likely because of the presence of strongly different metal atoms in the respective complexes. In contrast, the first cathodic peaks of **CuCl-1** ( $-0.42$  V) and **NiCl-1** ( $-0.22$  V) are visible at more positive potentials and can therefore be assigned to a metal-centered reduction.<sup>26</sup> Probably this is caused by the stronger in-plane coordination of Ni(II) and Cu(II) with a smaller deviation from the plane ( $0.32$  Å) compared to **MnCl-1**, **CoCl-1**, and **ZnCl-1** ( $0.53$ – $0.66$  Å). The quasireversible second reduction peaks of **MnCl-1**, **CoCl-1**, and **ZnCl-1** (not shown in Figure 4) appear at similar half wave potentials of  $-1.3$  V. Compared to the Fe(II)/Fe(III) redox process in **FeCl<sub>2</sub>-1** ( $0.595$  V),<sup>20</sup> the first oxidation potentials of the investigated complexes occur at more positive potential values and rise in the order Mn(II), Co(II), and Zn(II). **ZnCl-1** and **MnCl-1** undergo only one oxidation process while **CoCl-1** exhibits two anodic peaks. The first irreversible oxidation step of **CoCl-1** points to a possible chemical follow-up reaction to [Co(III)Cl-1]<sup>+</sup> or a kinetically hindered electron transfer process. The Co(II) complex of 5,10,15,20-tetraphenylporphyrin (**H<sub>2</sub>TPP**) features the same chemical behavior at  $0.52$  V in the first oxidation step to that discussed for Co(II)/Co(III) oxidation.<sup>51</sup> For **H<sub>2</sub>TPP** ( $E_{ox}^1 = 1.07$  V) it is known that the oxidation potential of the corresponding Zn(II) complex appears at lower values ( $E_{ox}^1 = 0.83$  V).<sup>52</sup> 21-Oxaporphyrin **1** and its Zn(II) complex show the opposite behavior. The estimated electrochemical gap for the complexes under study increases in the order Mn(II), Co(II), Zn(II). The addition of one electron to the LUMO becomes slightly easier in metal complexes.

Similar to the reported <sup>1</sup>H NMR spectra of Zn(II) oxaporphyrins,<sup>28</sup> **ZnCl-1** and **ZnClO<sub>4</sub>-2** show a downfield shift of almost all proton signals compared to their free base spectra. Due to the decreased symmetry, a splitting of the aryl proton signals is observed, in particular for the protons in the ortho-position. While the signals of the aryl rings adjacent to the furan ring are close to each other, the signals of the aryl rings adjacent to the pyrrole ring show a split of about  $0.4$  ppm (see Figure 5). In accordance with the results of the single crystal X-ray diffraction studies, this difference in the magnitude of splitting can be assigned to anion coordination deviating slightly from the vertical toward the pyrrole ring. Furthermore, the broadened signals of the aryl rings adjacent to the pyrrole become sharper upon cooling and coalesce upon heating, indicating a lower rotational energy barrier.<sup>28,53,54</sup>

The <sup>1</sup>H NMR spectrum of **ZnCl-3** shows signals in the phenylic region analogous to **ZnCl-1** and **ZnClO<sub>4</sub>-1**. The signals in the aliphatic region arising from the methyl and methylene groups can be classified into two signal sets, demonstrating the existence of two different complex species (A and B) in the solution. While one signal set is fairly similar to the free base spectrum, the other one shows strongly shifted and partially split signals (Figure 6, Table 5). Thus, the latter signal set can be assigned to a complex species in which the side chain functionality interacts with the metal center (species A).

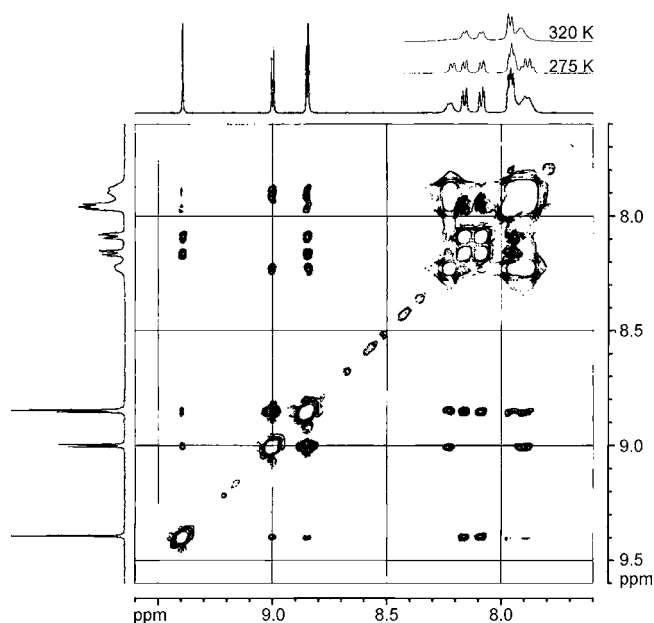


**Figure 5.** NOESY spectrum of **ZnClO<sub>4</sub>-2** in  $CDCl_3$  at 298 K. Dark spots display NOE signals and gray spots features proton exchange. The inset shows the changes of the aryl ring signals associated with temperature variation.

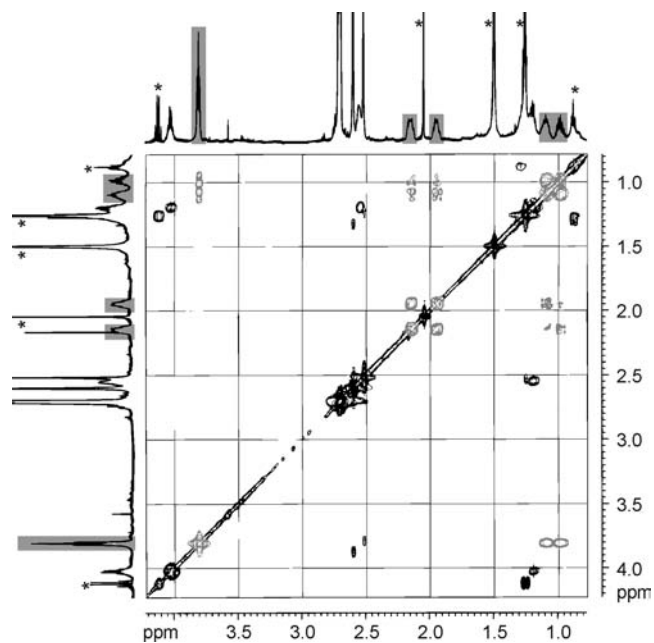


**Figure 6.** COSY spectrum of the aliphatic region of **ZnCl-3** in  $CDCl_3$  at 298 K. The peaks marked by asterisks belong to ethyl acetate and water. The gray highlighted signals are assigned to the side chain interacting with Zn(II).

Especially the upfield shifting of the diastereotopic methylene proton signals indicates that these protons are located above the porphyrin core. The other signal set arises from a species with no interaction between the fifth donor position and the zinc(II) central atom (species B). Due to an integral ratio of approximately 3:2 (A:B), species A can be assigned to be the preferred species in solution.

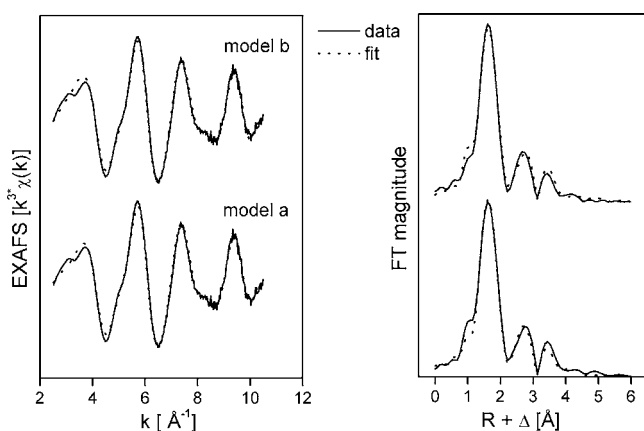
To obtain more information about the binding condition of Zn(II) in **ZnCl-3**, a Zn K-edge EXAFS spectrum of a solid

**Table 5.**  $^1\text{H}$  NMR Chemical Shifts of the Aliphatic Proton Signals of **3** and its Zn(II) Complex

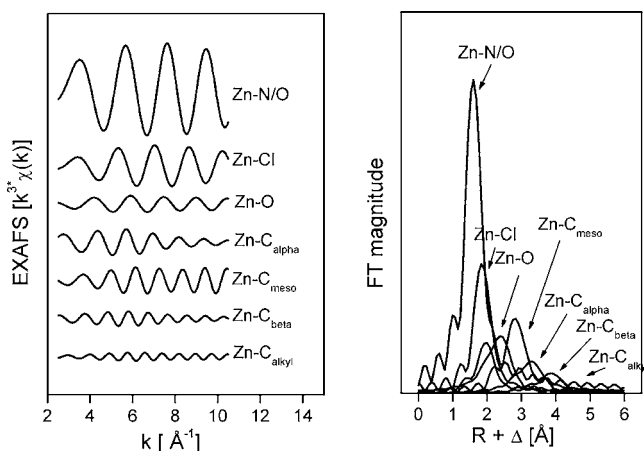
	<b>3</b>	ZnCl- <b>3</b>
m-Ar-CH <sub>3</sub>	2.55	2.60/2.50 <sup>a</sup>
OCH <sub>2</sub> CH <sub>2</sub> CH <sub>2</sub> OH	4.00	3.80/4.00 <sup>a</sup>
OCH <sub>2</sub> CH <sub>2</sub> CH <sub>2</sub> OH	1.20	1.00, 1.10/1.20
OCH <sub>2</sub> CH <sub>2</sub> CH <sub>2</sub> OH	2.70	1.95, 2.15/2.55 <sup>a</sup>
OH	not obsvd.	0.4/0.6 <sup>a</sup>

<sup>a</sup>Signals of the two species in the order coordinated/noncoordinated side chain.

sample was measured (Figure 7). The theoretical phase and amplitude function used in data analysis were calculated using

**Figure 7.** EXAFS spectra (left panel) and corresponding Fourier transforms (right panel) for models of the ZnCl-**3** complex.

X-ray data for ZnCl-**1**. The four shells found in the Fourier transform can be deconvoluted into either seven (model a, Figure 8) or six (model b) peaks (Table 6). According to model a, the

**Figure 8.** Deconvolution of different peaks obtained in the EXAFS spectrum and its corresponding Fourier transform of ZnCl-**3** according to model a.

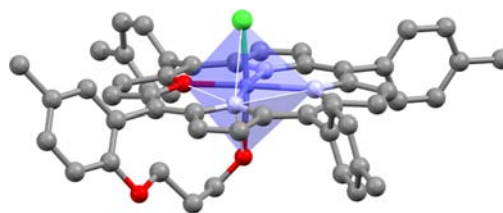
first shell, which is closest to Zn(II), splits into three components. The first two components can be assigned to the four donor atoms of the porphyrin (N<sub>3</sub>O) and the chloride with distances of 2.04 Å and 2.32 Å. The third peak at 2.45 Å corresponds to one oxygen atom and is most likely attributed to the OH group of the side chain. In general, Zn–O distances

**Table 6.** EXAFS Structural Parameters of the Zn(II) Complex of **3**

shell	N <sup>a</sup>	R [Å] <sup>b</sup>	σ <sup>2</sup> [Å <sup>2</sup> ] <sup>c</sup>	error <sup>d</sup>
model a				
Zn–N/O	4 <sup>f</sup>	2.04	0.0031	0.056
Zn–Cl	1 <sup>f</sup>	2.32	0.0051	0.056
Zn–O	1 <sup>f</sup>	2.45	0.0046	0.056
Zn–C <sub>alpha</sub>	8 <sup>f</sup>	3.05	0.014	0.056
Zn–C <sub>meso</sub>	4 <sup>f</sup>	3.36	0.0027	0.056
Zn–C <sub>beta</sub>	8 <sup>f</sup>	4.01	0.012	0.056
Zn–C/O <sub>alkyl chain</sub>	4 <sup>f</sup>	4.51	0.0065	0.056
model b				
Zn–N/O	4 <sup>f</sup>	2.04	0.0037	0.062
Zn–Cl	1 <sup>f</sup>	2.30	0.005	0.062
Zn–C <sub>alpha</sub>	8 <sup>f</sup>	3.04	0.013	0.062
Zn–C <sub>meso</sub>	4 <sup>f</sup>	3.36	0.0036	0.062
Zn–C <sub>beta</sub>	8 <sup>f</sup>	4.01	0.012	0.062
Zn–C/O <sub>alkyl chain</sub>	4 <sup>f</sup>	4.52	0.0072	0.062

<sup>a</sup>Errors in coordination numbers are  $\pm 25\%$ , and standard deviations as estimated by EXAFSPAK. <sup>b</sup>Errors in distance are  $\pm 0.02$  Å. <sup>c</sup>Debye–Waller factor. <sup>d</sup>Error is given as the normalized fit error  $\sum(\chi_{\text{data}}(k)k^3 - \chi_{\text{fit}}(k)k^3)^2 / (P - F)$  with  $P$  = number of data points,  $F$  = number of variables. <sup>e</sup>Fixed for calculation.

fall in a smaller range from 2.0 Å to 2.1 Å.<sup>55,56</sup> But longer distances of 2.47 Å or 2.71 Å<sup>57</sup> have also been reported. According to model b, this third peak has no structural origin and could be due to a side-lobe peak, originating from a truncation effect due to the limited reciprocal space integrated in the Fourier transform. The presence of such nonphysical shells using EXAFS spectroscopy is well documented, e.g., for uranyl ions with chloride.<sup>58,59</sup> Because both models are statistically equivalent best-fit models, the origin of the peak at 2.45 Å cannot be clarified unambiguously. However, compared to the crystal structure of ZnCl-**1** a reduction of the Zn–N/O distances and an enlargement of the Zn–Cl distance are observed. Both changes indicate that Zn(II) is closer to the plane defined by the four donor atoms of the porphyrin. This fact can be explained by the interaction with the additional donor function. As model a is also supported by the  $^1\text{H}$  NMR studies, an octahedral coordination geometry as shown in Figure 9 can be assumed for ZnCl-**3**.

**Figure 9.** Proposed structure of ZnCl-**3**.

Preliminary experiments of metal extraction from a metal salt mixture of Co(II), Ni(II), Cu(II), and Zn(II) perchlorates in aqueous solution with H<sub>2</sub>TPP and **1** dissolved in toluene showed a pronounced selectivity for Cu(II) and Zn(II). While both of the porphyrins extract Cu(II) quantitatively, the extraction of Zn(II) increases significantly on insertion of oxygen in the porphyrin core, from 58% to 99%, respectively. Compared to Cu(II) and Zn(II), the extraction of Co(II) and Ni(II) is very low (9–11%).

## CONCLUSIONS

Along with the synthesis of a pentadentate 21-oxaporphyrin, a convenient isolation procedure for oxaporphyrins is reported via the corresponding Zn(II) complex. A crucial feature of this procedure is the larger retention time obtained in comparison to the corresponding free base porphyrins, leading to improved chromatographic separation and isolation for the 21-oxaporphyrins.

Novel complexes of 21-oxaporphyrins have also been synthesized. Structural and electrochemical characterization of the Mn(II), Co(II), and Zn(II) tetraphenyl-21-oxaporphyrins (**MnCl-1**, **CoCl-1**, **ZnCl-1**) were performed, and the Cu(II) complex (**CuCl-1**) was characterized by X-ray diffraction for the first time. In all complexes investigated the metal center is coordinated by the four donor atoms of the oxaporphyrin and a chloride to give a square-pyramidal geometry. The electrochemical studies of Mn(II), Co(II), and Zn(II) oxaporphyrins exhibit redox behavior different from that of the known Cu(II) and Ni(II) complexes.

By introduction of a flexible side chain bearing a potential donor atom, the preference for octahedral coordination of Zn(II) could be verified via NMR and EXAFS studies. However, there is a chemical equilibrium of the two complex species with and without participation of the additional donor function in solution.

## EXPERIMENTAL SECTION

**Materials.** Column chromatography was carried out with silica gel 60 (0.040–0.063 mm Merck) or aluminum oxide 90 active basic (0.063–0.2 mm Merck). 2,5-Bis(phenylhydroxymethyl)furan (**1a**) and 5,10,15,20-tetraphenyl-21-oxaporphyrin (**1**) were synthesized as reported previously.<sup>17</sup> Crystals for X-ray diffraction were prepared by slow evaporation of the solvent from the metal complex solution in chloroform/*n*-heptane (2:1) for **CoCl-1**, **MnCl-1** or in chloroform/ethyl acetate (1:1) for **CuCl-1**, **ZnCl-1**.

**Instrumentation.** <sup>1</sup>H NMR spectra were measured on a Bruker DRX-500 at 500 MHz. The signals are described as s: singlet, d: doublet, m: multiplet, dd: double doublet, b: broad. UV/vis spectra were recorded on a Perkin-Elmer Lambda 2. The mass spectra were obtained on an Esquire Hewlett & Packard ESI-MS and a Shimadzu Kratos Kompact MALDI II mass spectrometer. The cyclic voltammograms were obtained with a PAR 273 potentiostat (EG&G, USA) in a three-electrode system using platinum wires as working and counter electrodes and a silver wire as pseudoreference electrode. Decamethylferrocene (dmFc) was added as internal standard. Dichloromethane (dried; Fluka), acetonitrile (puriss. absolute; Fluka), and dmFc (p.a.; Merck) were used as received. Tetrabutylammonium hexafluorophosphate (TBAPF<sub>6</sub>, Fluka, dried under reduced pressure at 340 K for 24 h prior to use; Fluka) was used as the supporting electrolyte. Elemental analysis was carried out with a CHNS element analyzer Hecatech EA 3000 Euro Vector. IR spectra were recorded on a Nicolet ATR Avatar 360. X-ray data for **CuCl-1** and **ZnCl-1** were collected at a Kappa APEX 2 diffractometer (Bruker-AXS). Solution and structure refinement calculations were performed by SHELXS-97 and SHELXL-97.<sup>60</sup> The C–Cl bond distances of the included solvent molecule in **CuCl-1** have been restrained to a target value of 1.70(1) Å. X-ray data for **MnCl-1** and **CoCl-1** were collected at a Kappa CCD diffractometer (Bruker-AXS). Zinc K-edge X-ray absorption spectra were collected from a solid sample in a KBr pellet at the Hamburger Synchrotronstrahlungslabor (HASYLAB Hamburg, Germany), Beamline E4. Measurements were performed by using a Si(111) double-crystal monochromator and Si-coated mirrors for focusing and rejection of higher harmonics. The data were collected in transmission mode using an Ar-flushed ionization chamber. The EXAFS oscillations were isolated from the raw, averaged data by removal of the pre-edge background, approximated by a first-order polynomial, followed by  $\mu 0$

removal via spline fitting techniques and normalization using a Victoreen function. The theoretical scattering phase and amplitude functions used in data analysis were calculated using FEFF7.<sup>61</sup> The shift in threshold energy,  $\Delta E_0$ , was varied as a global parameter in the fits. For extraction studies, H<sub>2</sub>TPP or **1** ( $5 \times 10^{-3}$  M) in toluene and a metal salt mixture of Co(ClO<sub>4</sub>)<sub>2</sub>, Ni(ClO<sub>4</sub>)<sub>2</sub>, Cu(ClO<sub>4</sub>)<sub>2</sub>, and Zn(ClO<sub>4</sub>)<sub>2</sub> (each  $1 \times 10^{-4}$  M) together with NaClO<sub>4</sub> ( $5 \times 10^{-3}$  M) was used. For pH adjustment a HEPES/NaOH buffer (pH = 6.9) was applied. The samples were stirred at 308 K for 24 h. The concentrations of metal ions in aqueous solution were determined by ICP-MS (ELAN-9000, Perkin-Elmer). **CAUTION.** Perchlorate complexes are potentially explosive and appropriate caution should be exercised in their handling.

**2,5-Bis[(4-bromophenyl)hydroxymethyl]-furan (2a).** In a three-necked, round-bottom flask with rubber septum and gas inlet tube tetramethylethylenediamine (1.9 mL, 0.01 mol) and furan (0.4 mL, 0.01 mol) were dissolved in 10 mL of dry hexane. After addition of an *n*-butyllithium solution (25 mL, 1.60 M in *n*-hexane) and refluxing for 1 h, the reaction mixture was cooled to 0 °C. A solution of 4-bromobenzaldehyde (1.85 g, 0.01 mol) in 30 mL of THF was added, and the mixture was stirred for another 10 min at room temperature. The reaction was quenched with saturated NH<sub>4</sub>Cl solution, and the aqueous layer was extracted with ethyl acetate. The combined organic layer was dried over Na<sub>2</sub>SO<sub>4</sub>, and the solvent was removed. The crude product was purified by column chromatography on silica gel using ethyl acetate/heptane (3:7) as eluent. The desired diol **2a** was obtained as the third fraction (1.07 g, 49%). <sup>1</sup>H NMR (CDCl<sub>3</sub>,  $\delta$  in ppm) 3.0 (s, 2H, OH), 5.5 (s, 2H, CH), 5.9 (d, 2H,  $\beta$ -furan-H), 7.2 (d, 4H, *o*-Ph-H), 7.4 (d, 4H, *m*-Ph-H).

**2-[(2-Methoxy-5-methylphenyl)hydroxymethyl]-5-[(*p*-tolyl)hydroxymethyl]-furan (3a).** Furan (3.6 mL, 0.05 mol) was dissolved in 10 mL of dry THF in a three-necked, round-bottom flask with rubber septum and gas inlet tube. An *n*-butyllithium solution (14.4 mL, 1.67 M in *n*-hexane) was added slowly, and the reaction mixture was refluxed for 1 h under slow argon purging. After cooling to 0 °C an ice cold solution of 2.0 mL (0.02 mol) of 4-methylbenzaldehyde in 10 mL of THF was added. The solution was stirred for 10 min at room temperature followed by quenching of the reaction with saturated NH<sub>4</sub>Cl solution. The organic layer was dried over Na<sub>2</sub>SO<sub>4</sub>, and the solvent was removed. The crude product was purified by column chromatography on silica gel using ethyl acetate/heptane (3:7) as eluent. The mono-ol, 2-[(4-methylphenyl)hydroxymethyl]-furan, was obtained as the second fraction in almost quantitative yield. <sup>1</sup>H NMR (CDCl<sub>3</sub>,  $\delta$  in ppm) 2.35 (s, 3H, CH<sub>3</sub>), 2.4 (s, 1H, OH), 5.8 (d, 1H, CH), 6.1 (d, 1H,  $\beta$ -furan-H), 6.3 (dd, 1H,  $\beta$ -furan-H), 7.2 (d, 2H, *m*-Ar-H), 7.3 (d, 1H, *o*-Ar-H), 7.4 (d, 1H,  $\beta$ -furan-H).

The mono-ol (3.00 g, 0.02 mol) was dissolved in 10 mL of dry THF in a three-necked, round-bottom flask with rubber septum and gas inlet. After cooling to 0 °C, *n*-butyllithium (28.6 mL, 1.67 M in *n*-hexane) was dropped slowly into the solution, and it was stirred for 1 h at 40 °C. The reaction mixture was cooled again to 0 °C and 2-methoxy-5-methyl-benzaldehyde in 10 mL of THF was added. After stirring for 10 min at room temperature and quenching with saturated NH<sub>4</sub>Cl solution, the organic layer was dried over Na<sub>2</sub>SO<sub>4</sub> and the solvent was removed. The crude product was purified by column chromatography on silica gel using ethyl acetate/heptane (3:7) as eluent. The desired diol **3a** was obtained as the third fraction (1.14 g, 21%). Due to the lability of the product, no NMR spectra could be recorded; the product was directly used for a cyclization reaction.

**5,10,15,20-Tetrakis(4-bromophenyl)-21-oxaporphyrin (2).** A solution of **2a** (1.34 g, 0.003 mol), 4-bromobenzaldehyde (1.10 g, 0.006 mol) and pyrrole (0.6 mL, 0.009 mol) in 1 L of dry dichloromethane was degassed and purged with argon. To start the condensation reaction, BF<sub>3</sub> diethyl etherate (0.04 mL, 0.3 mmol) was added, and the reaction mixture was stirred for 2 h in the dark under argon atmosphere at room temperature. After addition of 2,3-dichloro-5,6-dicyano-1,4-benzoquinone (DDQ) (1.36 g, 0.006 mol) and stirring on air for 10 h, the solvent was removed. The product **2** was purified by column chromatography on basic aluminum oxide (chloroform)



and obtained as a purple solid (0.42 g, 15%).  $^1\text{H}$  NMR ( $\text{CDCl}_3$ ,  $\delta$  in ppm)  $-1.7$  (s, 1H, NH),  $7.9$  (2 d, 8H, m-Ar-H),  $8.1$  (2 d, 8H, o-Ar-H),  $8.6$  (dd, 4H,  $\beta$ -pyrrolenine-H),  $8.9$  (s, 2H,  $\beta$ -pyrrole-H),  $9.2$  (s, 2H,  $\beta$ -furan-H); MALDI-MS obsd. mass 934, calcd. mass 930.9 (100%).

**5-(2-Methoxy-5-methylphenyl)-10,15,20-tri(*p*-tolyl)-21-oxaporphyrin (3b).** The oxaporphyrin 3b was prepared under the same experimental conditions as mentioned for 2. A solution of 3a (3.15 g, 0.009 mol), 4-methylbenzaldehyde (2.2 mL, 0.019 mol), and pyrrole (1.9 mL, 0.028 mol) in 2 L of dry dichloromethane and  $\text{BF}_3$  diethyl etherate (0.35 mL, 0.003 mol) was used. The oxidation was accomplished by addition of DDQ (2.11 g, 0.009 mol) and stirring in air for 10 h. For simplified separation the crude product was reacted to the zinc(II) complex by adding 10 equiv of  $\text{ZnCl}_2$  and brief heating. **ZnCl-3b** was obtained as a purple solid after column chromatography on silica gel (0.70 g, 0.81 mmol). Demetalation was achieved by treating **ZnCl-3b** in dichloromethane with conc. HBr solution (3 mL). The organic layer was washed with water and  $\text{NaHCO}_3$  solution. Column chromatography on basic aluminum oxide (dichloromethane/ethyl acetate 5:1) afforded the free base porphyrin 3b as purple solid (0.55 g, 9%).  $^1\text{H}$  NMR ( $\text{CDCl}_3$ ,  $\delta$  in ppm)  $-1.4$  (s, 1H, NH),  $2.6$  (s, 3H, m-Ar- $\text{CH}_3$ ),  $2.7$  (s, 9H, p-Ar- $\text{CH}_3$ ),  $3.6$  (s, 3H,  $\text{OCH}_3$ ),  $7.3$  (d, 1H, m-Ar-H),  $7.6$  (m, 7H, m/p-Ar-H),  $7.8$  (d, 1H, o-Ar-H),  $8.1$  (m, 6H, o-Ar-H),  $8.6$  (2 dd, 4H,  $\beta$ -pyrrolenine-H),  $8.9$  (2 d, 2H,  $\beta$ -pyrrole-H),  $9.2$  (2 d, 2H,  $\beta$ -furan-H); MALDI-MS obsd. mass 704, calcd. mass 701.3.

**5-[2-(3-Hydroxypropoxy)-5-methylphenyl]-10,15,20-tri(*p*-tolyl)-21-oxaporphyrin (3).** A solution of **ZnCl-3b** (0.21 g, 0.30 mmol) and  $\text{BBr}_3$  (0.13 mL, 1.30 mmol) in 10 mL of dry dichloromethane was stirred for 24 h at room temperature. After cooling to  $0^\circ\text{C}$ , 50 mL of water was added slowly to quench the reaction. The aqueous layer was adjusted to pH 6 using a NaOH solution (1 M) and extracted with ethyl acetate. The combined organic phases were dried over  $\text{Na}_2\text{SO}_4$  and the solvent was removed. The hydroxyl functionalized porphyrin 3c was purified by column chromatography on basic aluminum oxide (chloroform/ethyl acetate 20:1) and obtained as a purple solid (0.14 g, 79%).  $^1\text{H}$  NMR ( $\text{CDCl}_3$ ,  $\delta$  in ppm)  $2.6$  (s, 3H, m-Ar- $\text{CH}_3$ ),  $2.7$  (3 s, 9H, p-Ar- $\text{CH}_3$ ),  $7.3$  (d, 1H, m-Ar-H),  $7.6$  (m, 7H, m/p-Ar-H),  $7.8$  (s, 1H, o-Ar-H),  $8.1$  (m, 6H, o-Ar-H),  $8.7$  (m, 4H,  $\beta$ -pyrrolenine-H),  $8.9$  (s, 2H,  $\beta$ -pyrrole-H),  $9.3$  (d, 2H,  $\beta$ -furan-H); MALDI-MS obsd. mass 689, calcd. mass 687.3.

A solution of 3c (0.12 g, 1.80 mmol), 2-(3-bromopropoxy)-tetrahydro-2H-pyran (0.06 mL, 0.53 mmol),  $\text{K}_2\text{CO}_3$  (0.07 g, 0.53 mmol), and 18-crown-6 (0.001 g, 0.04 mmol) in dry acetonitrile was refluxed for 48 h. After removal of the solvent, the crude product was dissolved in dichloromethane. The solution was washed with water and dried over  $\text{Na}_2\text{SO}_4$ . The tetrahydro-2H-pyran (THP) protected porphyrin 3d was purified by column chromatography on basic aluminum oxide (chloroform/ethyl acetate 9:1) and obtained as purple solid (0.13 g, 86%).  $^1\text{H}$  NMR ( $\text{CDCl}_3$ ,  $\delta$  in ppm)  $-1.5$  (s, 1H, NH),  $1.5$ – $1.9$  (m, 8H,  $\text{OCH}_2\text{CH}_2\text{CH}_2\text{O}/\text{THP-CH}_2$ ),  $2.5$  (s, 3H, m-Ar- $\text{CH}_3$ ),  $2.7$  (3 s, 9H, p-Ar- $\text{CH}_3$ ),  $3.1$  (m, 2H,  $\text{OCH}_2$ ),  $3.5$  (m, 2H,  $\text{THP-OCH}_2$ ),  $4.0$  (m, 3H,  $\text{OCH}_2/\text{THP-CH}$ ),  $7.3$  (d, 1H, m-Ar-H),  $7.6$  (m, 7H, m/p-Ar-H),  $7.7$  (s, 1H, o-Ar-H),  $8.1$  (m, 6H, o-Ar-H),  $8.6$  (m, 4H,  $\beta$ -pyrrolenine-H),  $8.9$  (s, 2H,  $\beta$ -pyrrole-H),  $9.2$  (d, 2H,  $\beta$ -furan-H); MALDI-MS obsd. mass 831, calcd. mass 829.4.

Deprotection of the THP ether was done by treating a solution of 3d (0.13 g, 0.15 mmol) in 20 mL of chloroform/methanol (1:1) with *p*-toluenesulfonic acid monohydrate (0.11 g, 0.60 mmol) and a drop of water. The solution was stirred for 24 h at  $40^\circ\text{C}$ . The solvent was removed; the crude product was dissolved in chloroform and washed with water. Product 3 was isolated after column chromatography on silica gel (chloroform/methanol 9:1) as a purple solid (0.09 g, 80%).  $^1\text{H}$  NMR ( $\text{CDCl}_3$ ,  $\delta$  in ppm)  $1.20$  (m, 2H,  $\text{OCH}_2\text{CH}_2\text{CH}_2\text{OH}$ ),  $2.55$  (s, 3H, m-Ar- $\text{CH}_3$ ),  $2.70$  (m, 2H,  $\text{OCH}_2\text{CH}_2\text{CH}_2\text{OH}$ ),  $2.80$  (3 s, 9H, p-Ar- $\text{CH}_3$ ),  $4.00$  (m, 2H,  $\text{OCH}_2\text{CH}_2\text{CH}_2\text{OH}$ ),  $7.25$  (d, 1H, m-Ar-H),  $7.60$  (m, 7H, m/p-Ar-H),  $7.80$  (s, 1H, o-Ar-H),  $8.10$  (m, 6H, o-Ar-H),  $8.55$  (m, 4H,  $\beta$ -pyrrolenine-H),  $8.90$  (s, 2H,  $\beta$ -pyrrole-H),  $9.20$  (d, 2H,  $\beta$ -furan-H); IR 3500 (w, br,  $\nu\text{OH}$ ), 3233 (w,  $\nu\text{NH}$ ), 2920 (m,

$\nu\text{CH}$ ), 2856 (m,  $\nu\text{CH}$ ). MALDI-MS obsd. mass 748, calcd. mass 745.3.

**Chloro-(5,10,15,20-tetraphenyl-21-oxaporphyrinato)manganese(III) (MnCl-1).** A solution of 1 (0.05 g, 0.08 mmol) and  $\text{MnCl}_2\cdot 2\text{H}_2\text{O}$  (0.12 g, 0.80 mmol) in 20 mL of 1:1 chloroform/methanol was refluxed for 72 h. Product **MnCl-1** was purified by column chromatography on silica gel (ethyl acetate) and obtained as brown purple solid (0.06 g, quant.). ESI-MS obsd. mass 669.1 (M – Cl, 100%), calcd. mass 669.2 (M – Cl, 100%); Anal. Calcd C, 74.95; H, 4.00; N, 5.96. Found C, 73.10; H, 4.05; N, 5.58.

**Chloro-(5,10,15,20-tetraphenyl-21-oxaporphyrinato)cobalt(II) (CoCl-1).** A solution of 1 (0.05 g, 0.08 mmol) and  $\text{CoCl}_2\cdot 2\text{H}_2\text{O}$  (0.07 g, 0.40 mmol) in 20 mL of 1:1 chloroform/methanol was refluxed for 24 h. Product **CoCl-1** was purified by column chromatography on silica gel (ethyl acetate) and obtained as a brown purple solid (0.05 g, 85%). ESI-MS obsd. mass 673.1 (M – Cl, 100%), calcd. mass 673.2 (M – Cl, 100%); Anal. Calcd C, 74.53; H, 3.98; N, 5.93. Found C, 73.35; H, 4.10; N, 5.80.

**Chloro-(5,10,15,20-tetraphenyl-21-oxaporphyrinato)copper(II) (CuCl-1).** A solution of 1 (0.06 g, 0.09 mmol) and  $\text{CuCl}_2\cdot 2\text{H}_2\text{O}$  (0.15 g, 0.90 mmol) in 20 mL of 1:1 chloroform/methanol was refluxed for 24 h. Product **CuCl-1** was purified by column chromatography on silica gel (ethyl acetate) and obtained as a purple solid (0.06 g, quant.). ESI-MS obsd. mass 677.1 (M – Cl, 100%), calcd. mass 677.2 (M – Cl, 100%); Anal. Calcd C, 74.05; H, 3.95; N, 5.98. Found C, 73.00; H, 4.10; N, 5.66.

**Chloro-(5,10,15,20-tetraphenyl-21-oxaporphyrinato)zinc(II) (ZnCl-1).** A solution of 1 (0.15 g, 0.24 mmol) and  $\text{ZnCl}_2$  (0.17 g, 1.20 mmol) in 20 mL of 1:1 chloroform/methanol was refluxed for 24 h. Product **ZnCl-1** was purified by column chromatography on silica gel (ethyl acetate) and obtained as a purple solid (0.17 g, quant.).  $^1\text{H}$  NMR ( $\text{CDCl}_3$ ,  $\delta$  in ppm)  $7.7$  (bs, 2H, para-H),  $7.8$  (m, 10H, m/p-Ph-H),  $8.05$  (bd, 2H, o-Ph-H),  $8.2$  (d, 2H, o-Ph-H),  $8.3$  (d, 2H, o-Ph-H),  $8.35$  (bs, 2H, o-Ph-H),  $8.85$  (m, 4H,  $\beta$ -pyrrolenine/pyrrole-H),  $9.0$  (d, 2H,  $\beta$ -pyrrolenine-H),  $9.35$  (s, 2H,  $\beta$ -furan-H); ESI-MS obsd. mass 678.1 (M – Cl, 100%), calcd. mass 678.2 (M – Cl, 100%); Anal. Calcd C, 73.86; H, 3.94; N, 5.87. Found C, 72.15; H, 4.30; N, 5.20.

**Perchlorato-[5,10,15,20-tetrakis(4-bromophenyl)-21-oxaporphyrinato]zinc(II) (ZnClO<sub>4</sub>-2).** A solution of 2 (0.05 g, 0.05 mmol) and  $\text{Zn}(\text{ClO}_4)_2$  (0.06 g, 0.16 mmol) in 70 mL of 2:5 chloroform/methanol was refluxed for 24 h. Product **ZnClO<sub>4</sub>-2** was purified by column chromatography on silica gel (ethyl acetate) and obtained as a purple solid (0.06 g, quant.).  $^1\text{H}$  NMR ( $\text{CDCl}_3$ ,  $\delta$  in ppm)  $7.9$  (bm, 4H, o/m-Ph-H),  $7.95$  (m, 6H, m-Ph-H),  $8.1$  (d, 2H, o-Ph-H),  $8.15$  (d, 2H, o-Ph-H),  $8.22$  (bd, 2H, o-Ph-H),  $8.85$  (m, 4H,  $\beta$ -pyrrolenine/pyrrole-H),  $9.0$  (d, 2H,  $\beta$ -pyrrolenine-H),  $9.4$  (s, 2H,  $\beta$ -furan-H); ESI-MS obsd. mass 995.8 (M – Cl, 100%), calcd. mass 995.8 (M – Cl, 100%).

**Chloro-[5-[2-(3-hydroxypropoxy)-5-methylphenyl]-10,15,20-tri(*p*-tolyl)-21-oxaporphyrinato]zinc(II) (ZnCl-3).** A solution of 3 (0.09 g, 0.12 mmol) and  $\text{ZnCl}_2$  (0.16 g, 1.2 mmol) in 20 mL of 1:1 chloroform/methanol was refluxed for 24 h. Product **ZnCl-3** was purified by column chromatography on silica gel (ethyl acetate) and obtained as a purple solid (0.10 g, quant.).  $^1\text{H}$  NMR ( $\text{CDCl}_3$ ,  $\delta$  in ppm)  $0.4$  (bs, OH),  $0.6$  (bs, OH'),  $1.00$ – $1.10$  (m, 1.4H,  $\text{OCH}_2\text{CH}_2\text{CH}_2\text{OH}$ ),  $1.20$  (m, 0.6H,  $\text{OCH}_2\text{CH}_2\text{CH}_2\text{OH}'$ ),  $1.95$  and  $2.15$  (2 m, 2H,  $\text{OCH}_2\text{CH}_2\text{CH}_2\text{OH}$ ),  $2.50$  (s, 1H, m-Ar- $\text{CH}_3'$ ),  $2.55$  (m, 1H,  $\text{OCH}_2\text{CH}_2\text{CH}_2\text{OH}'$ ),  $2.60$  (s, 2H, m-Ar- $\text{CH}_3$ ),  $2.70$  (m, 9H, p-Ar- $\text{CH}_3$ ),  $3.80$  (t, 1.2H,  $\text{OCH}_2\text{CH}_2\text{CH}_2\text{OH}$ ),  $4.00$  (m, 0.8H,  $\text{OCH}_2\text{CH}_2\text{CH}_2\text{OH}'$ ),  $7.20$  (s, 1H, m-Ar-H),  $7.50$ – $7.65$  (m, 7H, m/p-Ar-H),  $7.90$  (bs, 2H, o-Ar-H),  $7.95$  (s, 1H, p-Ar-H),  $8.10$  (m, 1H, o-Ar-H),  $8.20$  (m, 1H, o-Ar-H),  $8.25$ – $8.30$  (bm, 2H, o-Ar-H),  $8.85$  (m, 4H,  $\beta$ -pyrrolenine/pyrrole-H),  $9.00$  (d, 2H,  $\beta$ -pyrrolenine-H),  $9.35$  (s, 2H,  $\beta$ -furan-H); MALDI-MS obsd. mass 810 (M – Cl, 100%), calcd. mass 808.3 (M – Cl, 100%); IR 3430 (w,  $\nu\text{OH}$ ), 3022 (w,  $\nu\text{CH}$ ), 2920 (m,  $\nu\text{CH}$ ).



## ■ ASSOCIATED CONTENT

## ■ Supporting Information

Crystallographic data. This material is available free of charge via the Internet at <http://pubs.acs.org>. These data can also be obtained free of charge from the CCDC (numbers 916565–916568) via [www.ccdc.cam.ac.uk/data\\_request/cif](http://www.ccdc.cam.ac.uk/data_request/cif), by emailing [data\\_request@ccdc.cam.ac.uk](mailto:data_request@ccdc.cam.ac.uk), or by contacting The Cambridge Crystallographic Data Center, 12, Union Road, Cambridge CB2 1EZ, UK; fax: +44 1223 336033.

## ■ AUTHOR INFORMATION

## Corresponding Author

\*E-mail: [karsten.gloe@chemie.tu-dresden.de](mailto:karsten.gloe@chemie.tu-dresden.de).

## Notes

The authors declare no competing financial interest.

## ■ ACKNOWLEDGMENTS

The authors would like to thank Steffen Seifert and the HASYLAB, Hamburg, Germany, for recording the EXAFS spectrum. Furthermore we are grateful for the determination of metal concentrations in aqueous solution by ICP-MS measurements at the Helmholtz Center Dresden-Rossendorf, Germany.

## ■ REFERENCES

- (1) Fowler, C. J.; Sessler, J. L.; Lynch, V. M.; Waluk, J.; Gebauer, A.; Lex, J.; Heger, A.; Zuniga-y-Rivero, F.; Vogel, E. *Chem.—Eur. J.* **2002**, *8*, 3485–3496.
- (2) Kral, V.; Kralova, J.; Kaplanek, R.; Briza, T.; Martasek, P. *Physiol. Res.* **2006**, *55*, S3–S26.
- (3) Chmielewski, P. J.; Latos-Grażyński, L.; Rachlewicz, K.; Glowiak, T. *Angew. Chem., Int. Ed. Engl.* **1994**, *33*, 779–781.
- (4) Furuta, H.; Asano, T.; Ogawa, T. *J. Am. Chem. Soc.* **1994**, *116*, 767–768.
- (5) Nakabuchi, T.; Matano, Y.; Imahori, H. *Org. Lett.* **2010**, *12*, 1112–1115.
- (6) Matano, Y.; Nakashima, M.; Nakabuchi, T.; Imahori, H.; Fujishige, S.; Nakano, H. *Org. Lett.* **2008**, *10*, 553–556.
- (7) Nakabuchi, T.; Nakashima, M.; Fujishige, S.; Nakano, H.; Matano, Y.; Imahori, H. *J. Org. Chem.* **2010**, *75*, 375–389.
- (8) Stepień, M.; Latos-Grażyński, L. *J. Am. Chem. Soc.* **2002**, *124*, 3838–3839.
- (9) Gupta, I.; Ravikanth, M. *Coord. Chem. Rev.* **2006**, *250*, 468–518.
- (10) Ulman, A.; Manassen, J. *J. Am. Chem. Soc.* **1975**, *97*, 6540–6544.
- (11) Ulman, A.; Manassen, J.; Frolow, F.; Rabinovich, D. *J. Am. Chem. Soc.* **1979**, *101*, 7055–7059.
- (12) Ulman, A.; Manassen, J. *J. Chem. Soc., Perkin Trans. 1* **1979**, 1066–1069.
- (13) Hill, R. L.; Gouterman, M.; Ulman, A. *Inorg. Chem.* **1982**, *21*, 1450–1455.
- (14) Ulman, A.; Manassen, J.; Frolow, F.; Rabinovich, D. *Inorg. Chem.* **1981**, *20*, 1987–1990.
- (15) Stein, P.; Ulman, A.; Spiro, T. G. *J. Phys. Chem.* **1984**, *88*, 369–374.
- (16) Broadhurst, M. J.; Grigg, R.; Johnson, A. W. *J. Chem. Soc. C* **1971**, 3681–3690.
- (17) Latos-Grażyński, L.; Pacholska, E.; Chmielewski, P. J.; Olmstead, M. M.; Balch, A. L. *Angew. Chem., Int. Ed. Engl.* **1995**, *34*, 2252–2254.
- (18) Latos-Grażyński, L. In *The Porphyrin Handbook*; Kadish, K. M., Smith, K. M., Guillard, R., Eds.; Academic Press: New York, 2000; Vol. 2, pp 361–417 and references cited therein.
- (19) Latos-Grażyński, L.; Chmielewski, P. J. *New J. Chem.* **1997**, *21*, 691–700.
- (20) Pawlicki, M.; Latos-Grażyński, L. *Inorg. Chem.* **2002**, *41*, 5866–5873.
- (21) Pawlicki, M.; Latos-Grażyński, L. *Inorg. Chem.* **2004**, *43*, 5564–5571.
- (22) Chmielewski, P. J.; Latos-Grażyński, L.; Olmstead, M. M.; Balch, A. L. *Chem.—Eur. J.* **1997**, *3*, 268–278.
- (23) Gross, Z.; Saltsman, I.; Pandian, R. P.; Barzilay, C. M. *Tetrahedron Lett.* **1997**, *38*, 2383–2386.
- (24) Pacholska, E.; Chmielewski, P. J.; Latos-Grażyński, L. *Inorg. Chim. Acta* **1998**, *273*, 184–190.
- (25) Chmielewski, P. J.; Latos-Grażyński, L. *Inorg. Chem.* **1998**, *37*, 4179–4183.
- (26) Sridevi, B.; Narayanan, S. J.; Srinivasan, A.; Chandrashekar, T. K.; Subramanian, J. *J. Chem. Soc., Dalton Trans.* **1998**, 1979–1984.
- (27) Kumaresan, D.; Santra, S.; Ravikanth, M. *Synlett* **2001**, 1635–1637.
- (28) Ambre, R.; Yu, C.-Y.; Mane, S. B.; Yao, C.-F.; Hung, C.-H. *Tetrahedron* **2011**, *67*, 4680–4688.
- (29) Ghosh, A.; Ravikanth, M. *Inorg. Chem.* **2012**, *51*, 6700–6709.
- (30) Cho, W.-S.; Kim, H.-J.; Littler, B. J.; Miller, M. A.; Lee, C.-H.; Lindsey, J. S. *J. Org. Chem.* **1999**, *64*, 7890–7901.
- (31) Gonzalez, B.; Kouba, J.; Yee, S.; Reed, C. A.; Kirner, J. F.; Scheidt, W. R. *J. Am. Chem. Soc.* **1975**, *97*, 3247–3249.
- (32) Madura, P.; Scheidt, W. R. *Inorg. Chem.* **1976**, *15*, 3182–3184.
- (33) Fleischer, E. B. *J. Am. Chem. Soc.* **1963**, *85*, 1353–1354.
- (34) Scheidt, W. R.; Mondal, J. U.; Eigenbrot, C. W.; Adler, A.; Radonovich, L. J.; Hoard, J. L. *Inorg. Chem.* **1986**, *25*, 795–799.
- (35) Scheidt, W. R. *J. Am. Chem. Soc.* **1974**, *96*, 90–94.
- (36) Dwyer, P. N.; Madura, P.; Scheidt, W. R. *J. Am. Chem. Soc.* **1974**, *96*, 4815–4819.
- (37) Scheidt, W. R.; Ramanuja, J. A. *Inorg. Chem.* **1975**, *14*, 2643–2648.
- (38) Glick, M. D.; Cohen, G. H.; Hoard, J. L. *J. Am. Chem. Soc.* **1967**, *89*, 1996–1998.
- (39) Reid, H. O. N.; Kahwa, I. A.; White, A. J. P.; Williams, D. J. *Inorg. Chem.* **1998**, *37*, 3868–3873.
- (40) Mohamadou, A.; Jubert, C.; Barbier, J.-P. *Inorg. Chim. Acta* **2006**, *359*, 273–282.
- (41) Amini, M. M.; Yadavi, M.; Ng, S. W. *Acta Crystallogr., Sect. E: Struct. Rep. Online* **2004**, *60*, m492–m494.
- (42) Denmark, S. E.; Edwards, J. P.; Wilson, S. R. *J. Am. Chem. Soc.* **1992**, *114*, 2592–2602.
- (43) Cheng, B.; Scheidt, W. R. *Acta Crystallogr., Sect. C: Cryst. Struct. Commun.* **1996**, *C52*, 361–363.
- (44) Iimura, Y.; Sakurai, T.; Yamamoto, K. *Bull. Chem. Soc. Jpn.* **1988**, *61*, 821–826.
- (45) Antonioli, B.; Buchner, B.; Clegg, J. K.; Gloe, K.; Gloe, K.; Götzke, L.; Heine, A.; Jäger, A.; Jolliffe, K. A.; Kataeva, O.; Kataev, V.; Klingeler, R.; Krause, T.; Lindoy, L. F.; Popa, A.; Seichter, W.; Wenzel, M. *Dalton Trans.* **2009**, 4795–4805.
- (46) OTMPP refers to 5,10,15,20-tetrakis[4-(methoxycarbonyl)phenyl]-21-oxaporphyrin.
- (47) ODPDTP refers to 10,15-diphenyl-5,20-di(p-tolyl)-21-oxaporphyrin.
- (48) Steiner, T. *Angew. Chem.* **2002**, *114*, 50–80.
- (49) Dorough, G. D.; Miller, J. R.; Huennekens, F. M. *J. Am. Chem. Soc.* **1951**, *73*, 4315–4320.
- (50) Sridevi, B.; Narayanan, S. J.; Srinivasan, A.; Reddy, M. V.; Chandrashekar, T. K. *J. Porphyrins Phthalocyanines* **1998**, *2*, 69–78.
- (51) D'Souza, F.; Villard, A.; Van Caemelbecke, E.; Franzen, M.; Boschi, T.; Tagliatesta, P.; Kadish, K. M. *Inorg. Chem.* **1993**, *32*, 4042–4048.
- (52) Huang, C.-W.; Yuan Chiu, K.; Cheng, S.-H. *Dalton Trans.* **2005**, 2417–2422.
- (53) Latos-Grażyński, L.; Lisowski, J.; Chmielewski, P.; Grzeszczuk, M.; Olmstead, M. M.; Balch, A. L. *Inorg. Chem.* **1994**, *33*, 192–197.
- (54) Eaton, S. S.; Eaton, G. R. *J. Am. Chem. Soc.* **1975**, *97*, 3660–3666.
- (55) Trainor, T. P.; Braun, G. E., Jr.; Parks, G. A. *J. Colloid Interface Sci.* **2000**, *231*, 359–372.
- (56) Langford, S. J.; Woodward, C. P. *Polyhedron* **2007**, *26*, 338–343.

- (57) Iitaka, Y.; Oswald, H. R.; Locchi, S. *Acta Crystallogr.* **1962**, *15*, 559–563.
- (58) Servaes, K.; Hennig, C.; van Deun, R.; Görrler-Walrand, C. *Inorg. Chem.* **2005**, *44*, 7705–7707.
- (59) Hennig, C.; Tutschku, J.; Rossberg, A.; Bernhard, G.; Scheinost, A. C. *Inorg. Chem.* **2005**, *44*, 6655–6661.
- (60) (a) Sheldrick, G. M. *Acta Crystallogr.* **1990**, *A46*, 467–473.  
(b) Sheldrick, G. M. *SHELXL97*; University of Göttingen: Göttingen, Germany, 1997.
- (61) Ankudinov, A. L.; Ravel, B.; Rehr, J. J.; Conradson, S. D. *Phys. Rev. B* **1998**, *58*, 7565–7575.